RF Sputtered Strontium Titanate Films

Abstract: Two deposition parameters are important in rf sputtering of $SrTiO_3$ films: the oxygen-argon content ratio, and the substrate temperature. More than 1% oxygen is needed to produce insulating films; the exact percentage required depends on system cleanliness. Both dielectric constant and crystallite size increase with increasing substrate temperature.

Films of 2400 Å deposited at 500° C on gold have a dielectric constant of 200. The dc conductivity closely follows the Poole-Frenkel model. Two dielectric loss peaks are believed to be caused in part by an oxygen deficient region near one electrode. The variation in the dielectric constant κ with electric field is similar to that observed in bulk material.

Introduction

The deposition of SiO₂ films by rf sputtering has been extensively investigated by a number of researchers. The dielectric properties of sputtered SiO₂ are generally excellent, being influenced in rather subtle ways by changes in deposition parameters. Sputtering of SrTiO₃ is quite different. As will be shown, the dielectric properties of rf sputtered SrTiO₃ films are extremely sensitive to two of the sputtering parameters, substrate temperature and oxygen partial pressure. The sensitivity to these parameters arises through their influence on oxygen deficiency and crystalline perfection.

A brief review of the room temperature properties of bulk SrTiO₃ is in order. SrTiO₃ has a cubic perovskite structure.¹ Its dielectric constant² is about 300, resulting primarily from an optical mode which resonates³ at 87.5 cm⁻¹ (2.6 \times 10¹² Hz). Dielectric loss⁴ is observed at lower frequencies in two broad ranges, one below 10⁴ Hz, the other from 10⁴ Hz to >10⁷ Hz. SrTiO₃ is readily reduced, the resulting oxygen vacancies acting as very shallow donors.⁵ At room temperature over a wide doping range, the free carrier single crystal mobility⁶ is \approx 5 cm²/V-sec.

Sputtering techniques and equipment

In this section the sputtering equipment and its operation will be described. Particular emphasis will be given to the problems associated with the addition of oxygen to the sputtering gas.

The sputtering system arrangement followed a conventional⁶ diode design. The vacuum system consisted of a standard Edwards six-inch mercury diffusion pump with liquid nitrogen and Freon baffles. A Varian bellows-sealed right angle gate valve connected the pumping system to a stainless steel "T" where the sputtering was done. Roughing was done through a liquid nitrogen trapped line. A Veeco GA-3 mass spectrometer connected between the gate valve and the pumping system monitored gas composition during sputtering. The main gate valve was closed during sputtering; a two-inch bypass valve was adjusted to provide a pressure of 5 to 10 millitorr in the sputtering chamber, while a pressure of 5×10^{-5} torr was maintained in the section with the mass spectrometer. At this pressure, the mass spectrometer sensitivity was slightly reduced. Much larger changes in sensitivity occurred when oxygen was introduced into the mass spectrometer. These effects were carefully accounted for in the gas analysis.

The target* was pressed and fired by standard techniques from technical grade $SrTiO_3$. The analysis provided by the supplier indicated a total impurity content of about 5.4%. The major impurities were: 1.25% SiO_2 , 1.00% Al_2O_3 , 0.5% CaO, 0.5% MgO, 0.75% CaO and 0.75% CaO NaKO. Target outgassing was not a problem. The system base pressure was $C_3 \times 10^{-8}$ torr.

Substrate temperatures between 200°C and 500°C were investigated. The substrates, 0.025 cm thick, 2.5 cm diameter sapphire disks† coated with various metal films,

The author is located at the IBM Thomas J. Watson Research Center, Yorktown Heights, New York.

^{*} Purchased from American Lava Corp., Chattanooga, Tenn.

[†] Purchased from Insaco, Inc., Quakertown, Pa.

were clamped to the temperature controlled holder with gallium at the interface to ensure good thermal contact. The holder was made of molybdenum with tungsten disks brazed to it to support the substrates. Tungsten does not interact with gallium at 500°C.⁷ The holder was heated from the back by radiation from a Pt-13% Rh filament.

As noted earlier, substrate temperature and oxygen partial pressure were the two important deposition parameters. Changes in rf power, magnetic field (supplied by two Helmholtz coils), total gas pressure,* anodecathode spacing, and dc bias on the substrate holder changed the deposition rate, but not (to first order) the film properties. All the samples described in this paper were deposited using standard conditions listed in Table 1. Film thicknesses ranged from 1400 Å to 7300 Å.

The only parameter listed in Table 1 that could not be accurately controlled was the oxygen partial pressure. The problem is illustrated in Fig. 1. The pressures plotted in Fig. 1 were the ion gauge pressures calculated from the peaks recorded by the mass spectrometer; they were proportional to the partial pressures in the sputtering chamber, but the proportionality constants depended on the throttled gate valve conductances which were different for the different gases. The startling feature (apparent in Fig. 1) was the conversion of most of the oxygen to carbon monoxide[†] during the initial moments of the run. The source of the carbon was hydrocarbons adsorbed on the walls of the system during exposure to room air. This was proved in a series of experiments in which the duration of system exposure to air was varied. With no air exposure (system raised to atmospheric pressure with argon) no CO was evolved. One half hour of air exposure produced the effect seen in Fig. 1. Exposure for 16 hours gave an effect which persisted through several runs. Hydrogen and water vapor also were evolved initially, in a manner very similar to that of CO. However, their partial pressures were more than an order of magnitude smaller than the CO pressure, and were not changed when the shutter was opened. The increase in CO partial pressure that occurred upon opening the shutter suggests that carbon contaminated the fully outgassed substrate holder. It should be noted that similar, but far smaller, CO evolution has been observed at hot tungsten filaments.²⁵

The presence of CO was not harmful, in that films deposited in argon, 10% oxygen, 10% CO were not significantly altered by this deliberate contamination. (Normally, the CO pressure was less than 1% of the total during film deposition.) The reaction between oxygen and hydrocarbons, however, made control of low oxygen concentrations (less than 5%) quite difficult. For this reason the data on the effect of oxygen pressure are qualitative.

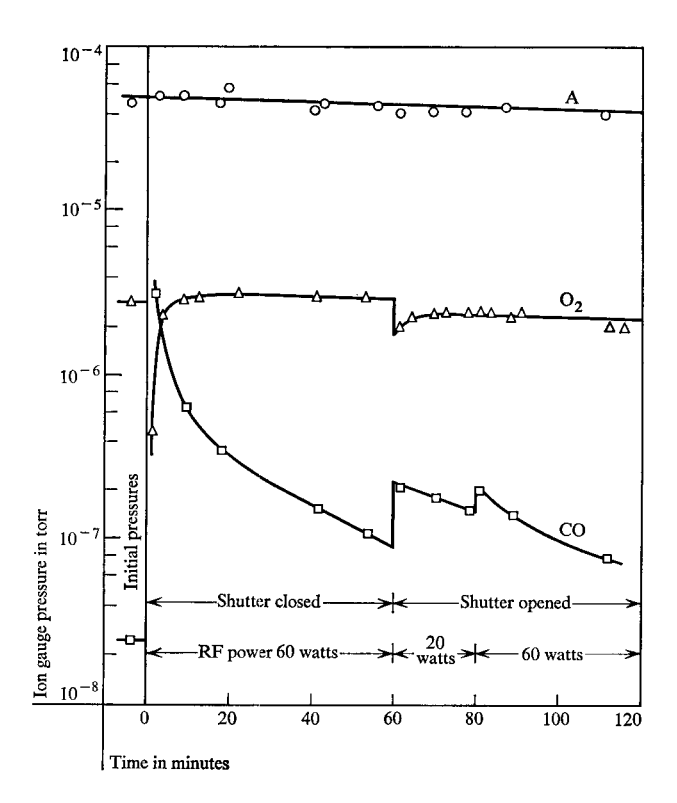


Figure 1 Partial pressures during sputtering.

Table 1 Sputtering conditions.

RF power during deposition ^a	60 to 100 watts
Magnetic field (axial)	60 gauss
Total discharge pressure	5 to 10 millitorr
Substrate temperature	200 to 500°C as desired
Oxygen concentration (in argon)	0 to 100%—see text
Anode-cathode spacing	2.5 cm
Cathode diameter	10 cm
Clean-up before opening shutter	60 minutes at deposition power
Substrate bias	Floating ($\approx -30 \text{ volts}$)
Deposition rate (for O ₂	- '
concentration $> 1\%$)	$\approx 30 \text{ Å/minute}$
Base pressure of system	1 to 5 \times 10 ⁻⁸ torr

^a To improve control of the various parameters the rf power was reduced to 20 watts just prior to opening the shutter and held at this level for the first 20 minutes of film deposition.

Once the discharge was struck, the oxygen in the system was far more reactive. This produced the evolution of CO; it also caused significant oxidation of other materials exposed to the discharge. In the first experiments, clean silicon wafers were used as substrates in place of the metallized sapphire. It was found, in comparing with later films deposited on gold, that the equivalent of approximately 100 Å of SiO₂ grew during the deposition of a 2500 Å film of SrTiO₃. The SiO₂ growth seemed to be independent of substrate temperature. Although the

^{*} Except as this affected oxygen partial pressure.

[†] The carbon monoxide was uniquely identified through its cracking pattern.

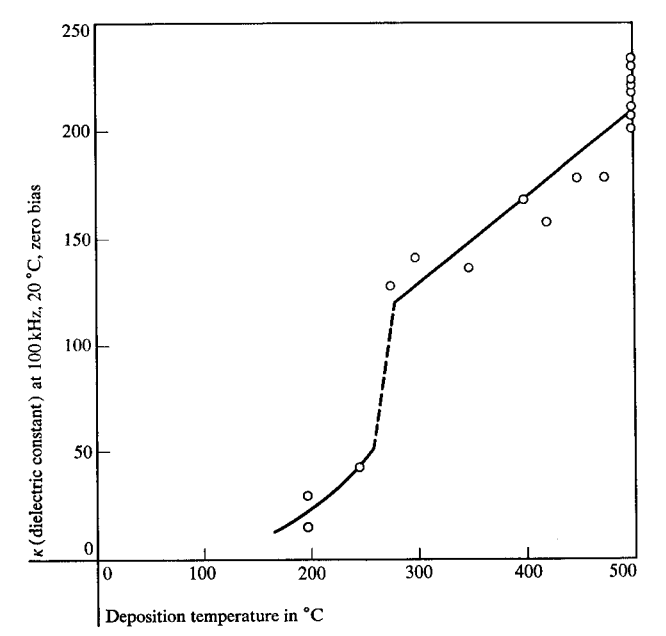


Figure 2 Dependence of κ on deposition temperature.

films on silicon had curious capacitance-voltage characteristics, the series layer of low-dielectric-constant silicon oxide obscured the properties of the SrTiO₃ itself. SrTiO₃ was deposited on films of Au, Cu, Ag, Ti, Ta, Mo, W, and Pt. All except Pt and Au oxidized sufficiently to mask the properties of the SrTiO₃; some (Cu, Ta) were converted completely to their oxides. Pt reacted in a different and adverse way with SrTiO₃, the surface becoming so rough that the SrTiO₃ was shorted. This was presumably the same reaction⁸ that occurs when SrTiO₃ is fired in contact with Pt.

Only Au showed no reaction with the oxygen or SrTiO₃. Therefore, in all samples to be described in this paper, the SrTiO₃ was deposited on Au-Mo-sapphire structures.

The Au films did have one problem, a growth of micronsized hillocks due to compressive stress in the Au at 500°C. This has been fully described in a recent publication. To minimize this growth, the substrate holder was outgassed at 200°C during pumpdown. The substrates were heated to 500°C only for the actual film deposition.

Counter electrodes were formed with sputtered films of Mo and Cu, and evaporated films of Al. The Al electrode structures had high leakage currents. Since faint signs of cracking of the SrTiO₃ were observed near these Al electrodes, this structure was not investigated further.

Film properties

This section describing film properties will be divided into five parts. First, those properties that depend on the deposition parameters in a direct manner will be discussed. The second part will present dielectric loss measurements. The third part will analyze the dc conduction in highly insulating films. The fourth part will present the heat treatment and electrode dependent effects. The fifth and final part will describe the variation of the dielectric constant with electric field.

• Film properties depending directly on deposition parameters

As noted earlier, two deposition parameters, substrate temperature and oxygen partial pressure, were the main factors determining the properties of the $SrTiO_3$ films. The difficulty in controlling small oxygen partial pressures made it impossible to obtain complete data on this parameter. However, the following general observations can be made: Films deposited in pure argon were dark, almost metallic in appearance, and conducted readily. When about 1% oxygen was added to the argon, a poorly insulating film resulted. With more than 5% oxygen in the argon, the film had a high resistivity and a breakdown field greater than 10^6 volts/cm.

These qualitative results are in agreement with the properties of bulk SrTiO₃, in that an oxygen deficient material will conduct readily. In earlier, unpublished work, H. Caswell and the author used the apparatus described in this paper to measure crudely the amount of oxygen lost from SiO₂ during sputtering. The loss was not large, only about 0.25%. However, if this much oxygen was lost from SiO₂ during sputtering, it is not surprising that SrTiO₃ (which is more readily reduced) formed conducting films when sputtered in pure argon. The conductivity of the insulating SrTiO₃ films will be discussed more fully later in this paper.

Although oxygen partial pressure was a strong factor in determining film resistivity, the high frequency (> 100 kHz) dielectric constant κ was essentially independent of that sputtering parameter. What did influence the dielectric constant was deposition temperature. Figure 2 gives an idea of its effect. The exact variation of κ with deposition temperature is a function of both the temperature and the frequency at which the measurement is made. However, the dependence on these parameters is relatively small,* and Fig. 2 presents the essential picture.

It is of interest to know what structural changes occurred as the deposition temperature was changed. The films were too thin (2000 Å to 3000 Å typically) for x-ray diffraction analysis. However, 1000 Å films could be removed for examination by dissolving the Au in aqua regia. These unsupported structures were analyzed by transmission electron microscopy; the results are shown in Fig. 3. The micrographs clearly show an increase in grain size with increasing deposition temperature. This

[•] In the discussion which follows, care should be taken to distinguish between the two different temperatures, deposition temperature and measurement temperature.

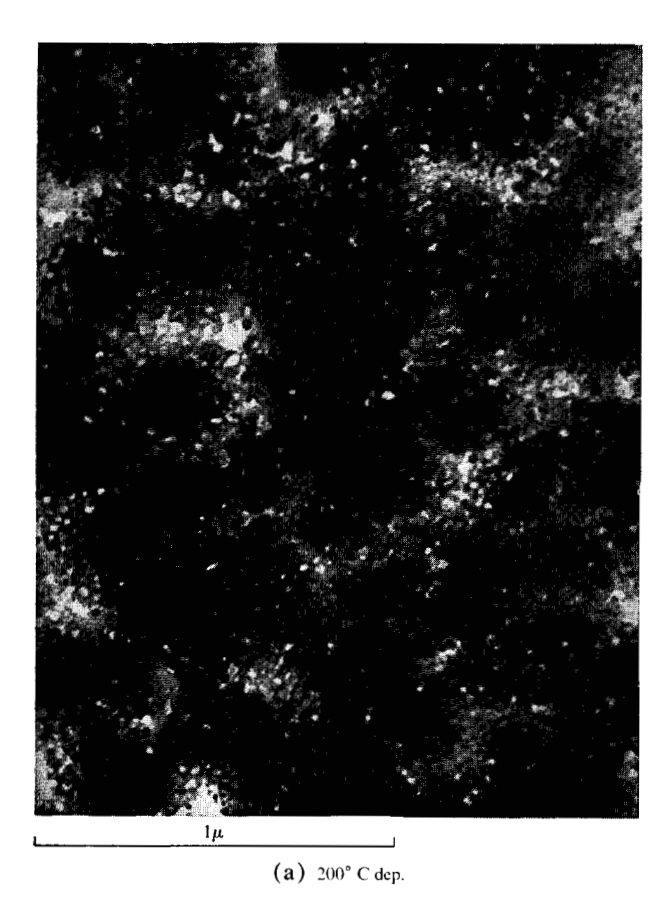


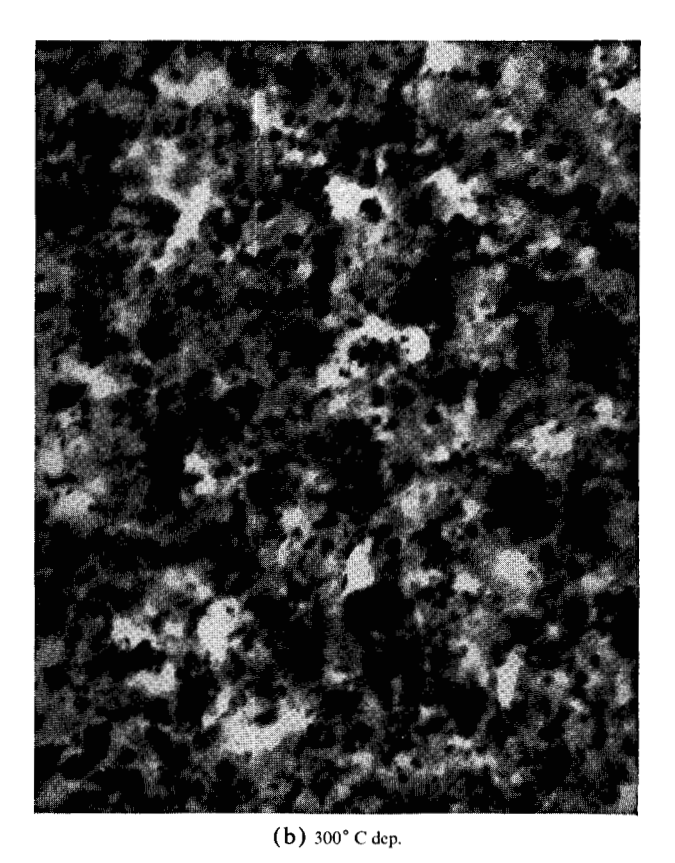
Figure 3 Transmission electron micrographs of 1000 Å films deposited at (a) 200°C, (b) 300°C and (c) 500°C.

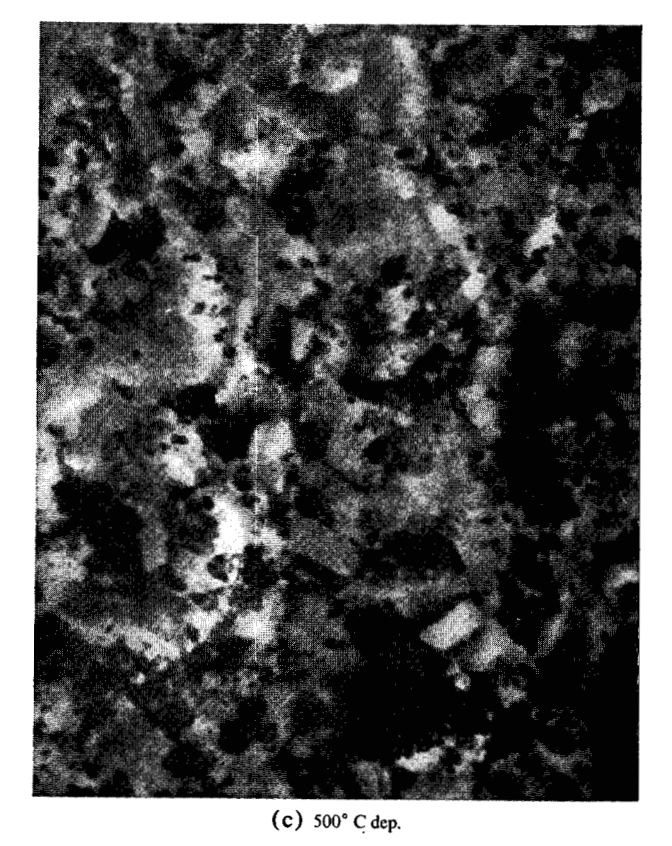
was accompanied by a sharpening of the electron diffraction pattern. It is significant that only SrTiO₃ lines were found in the diffraction patterns; x-ray fluorescence and chemical analysis also gave qualitative indication of a correct Sr-Ti ratio in the films.

Dielectric loss

The dielectric loss in these films was a complex function of a number of variables: oxygen pressure during sputtering, deposition temperature, film thickness, electrode material, and the temperature and bias during measurement. However, changes in the relative humidity of the ambient during measurement did not affect either κ or dielectric loss. Because of the complexity, considerably more work remains to be done before a full understanding can be reached.

Figure 4 gives a set of loss curves measured without de bias for a 2400 Å thick SrTiO₃ film deposited at 500°C in 10% oxygen. The data illustrate a feature common to virtually all the films: a distinct minimum between low frequency and high frequency regions of loss. Not surprisingly, the loss was much larger in oxygen deficient films. A similarly larger loss was encountered when Mo





689

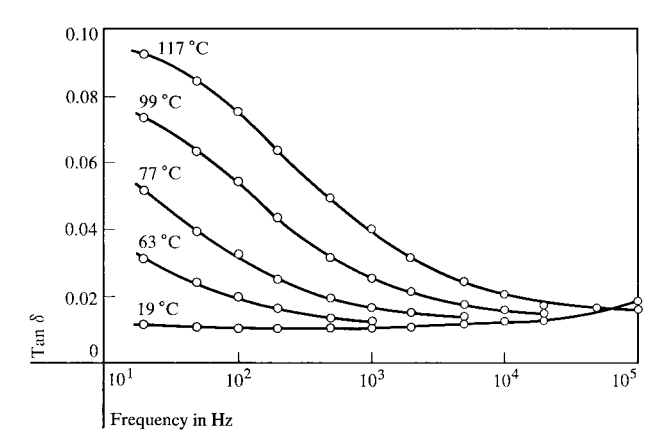


Figure 4 Dielectric loss in a typical SrTiO₃ film deposited at 500°C with 10% oxygen added to the sputtering gas (film thickness 2400 Å).

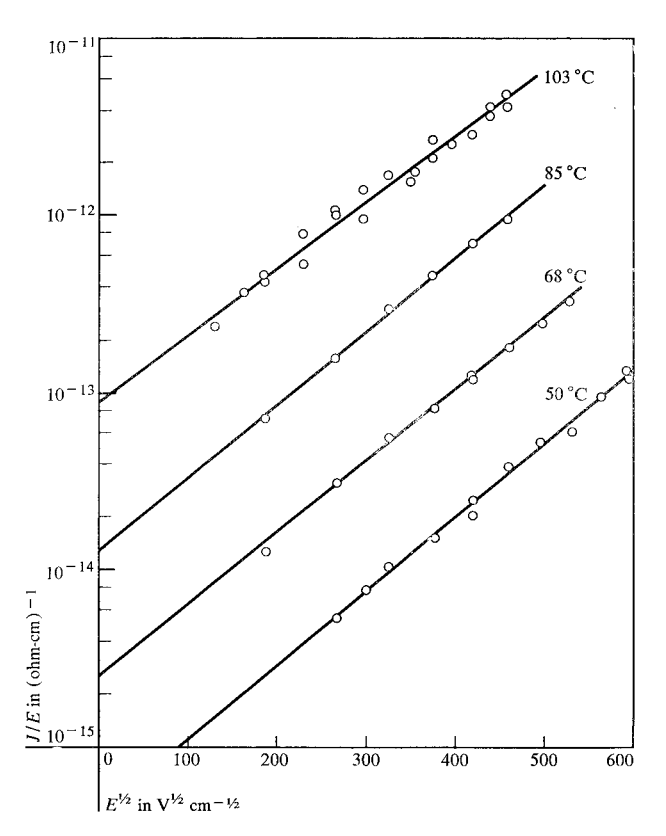


Figure 5 Conduction in the forward direction, Cu negative.

was used in place of Cu as the top electrode. This is also believed to be an oxygen deficiency effect, caused by the formation of molybdenum oxide at the expense of the SrTiO₃ oxygen content. Further evidence for the relation between electrode material and oxygen deficiency will be given in the discussion of dc conductivity.

Although oxygen content was an important factor, the dielectric loss in highly oxidized films was far too large to

be due to shunting dc conduction. An important insight into at least part of the loss mechanism was gained when it was discovered that (throughout the range of measurement) the loss decreased with increasing film thickness.* This indicated an inhomogeneity in the film: a region of higher loss associated with at least one boundary. Such a region could have been created by surface reduction of the film immediately following the deposition. At that point, the film was exposed to a relatively low pressure environment while still at 500°C. The surface of single crystal SrTiO₃ is known to reduce under these conditions. ¹⁰ It is also known that oxygen diffusion is enhanced if the SrTiO₃ is polycrystalline. ¹¹

The effective capacitance at very high frequencies was measured by using typical structures to terminate $50-\Omega$ coaxial lines. The capacitance inferred from the charging rate following reflection of a 0.2 nsec risetime pulse was essentially the same as measured at 100 kHz. Thus, dielectric loss was small between 10^5 Hz and about 10^9 Hz. On the other hand, slowly decaying transient currents were observed during the measurement of the dc characteristics, evidence for additional very low frequency loss. This could well have been caused by the blocking contact that is known to exist between the SrTiO₃ and the Au base film.¹⁷ This mechanism was proposed as an explanation of the dielectric loss in bulk SrTiO₃.⁴

The low frequency dielectric loss was greatly decreased as the deposition temperature was lowered, except in the two films deposited at 200°C. Since the Cu top electrode was deposited at 250°C, there is reason to suspect that the subsequent electrode deposition influenced the loss in those films. While it is tempting to ascribe the change in loss with deposition temperature to a change in surface reduction, the thickness dependence of loss has not been established at the lower deposition temperatures.

• DC conductivity

Order-of-magnitude differences in dc conductivity were encountered among various samples. The problem stemmed from defective regions in the SrTiO₃ caused by hillocks¹⁰ and other protrusions from the underlying gold film. To circumvent this problem, a method was devised to etch away the top electrode near these defective regions and thus isolate them. A thin layer of Shipley AZ-1350 photoresist was spun onto the 5000 Å thick copper film using standard techniques. The sample was then immersed in 25% HNO3. After a short time, usually about one minute, the copper film began to show etching wherever there was a protrusion large enough to cause a flaw in the photoresist. This process usually eliminated shorts, and worked well enough in a few cases to allow the measurement of the intrinsic conductivity. These measurements will be described in the next paragraphs.

^{*} The frequency dependence was also altered.

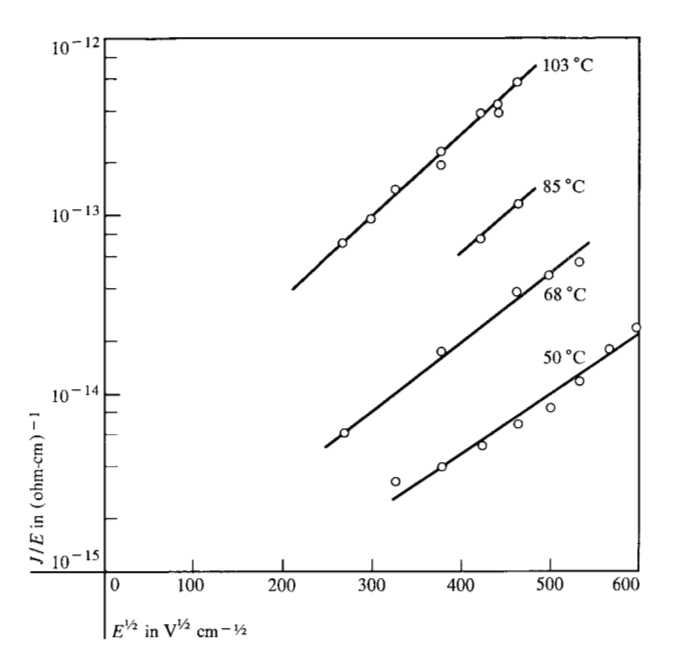


Figure 6 Conduction in the reverse direction, Cu positive.

Reliable and reproducible data were taken on films deposited at 500°C in 10% oxygen. The current-field dependence was non-ohmic and asymmetric in the Cu-SrTiO₃-Au structure, indicating at least one blocking electrode. Below 50°C, the transient current decayed so slowly that reliable steady state measurements could not be made. Above about 100°C, oxidation of the copper made the contact there uncertain; dielectric breakdown also restricted the range of applied field at higher temperatures. Thus, the temperature range of the data was necessarily limited. The conduction was not affected by a change in ambient from room air to dry nitrogen; it was also not affected by visible light. Reproducibility of the data from electrode to electrode was good ($\approx \pm 10\%$) for a given SrTiO₃ film, but differences almost as large as an order of magnitude were found among different films. Data taken on a typical film are given in Figs. 5 and 6 for the two directions of current flow.

Figure 5 shows that conduction in the easy direction had the field dependence expected¹² for the Poole-Frenkel mechanism*:

$$J = \sigma_0 E \exp(-\epsilon_d/kT) \exp(\beta_{pf} E^{\frac{1}{2}}/kT);$$

$$\beta_{pf} = (7.6/n) \times 10^{-4} \text{ eV-cm}^{\frac{1}{2}} \text{ V}^{-\frac{1}{2}}.$$
 (1)

There is controversy in the literature regarding the value of β_{pf} . Mark and Hartman¹³ demonstrated, however, that the expressions in Eq. (1) are valid for the most likely

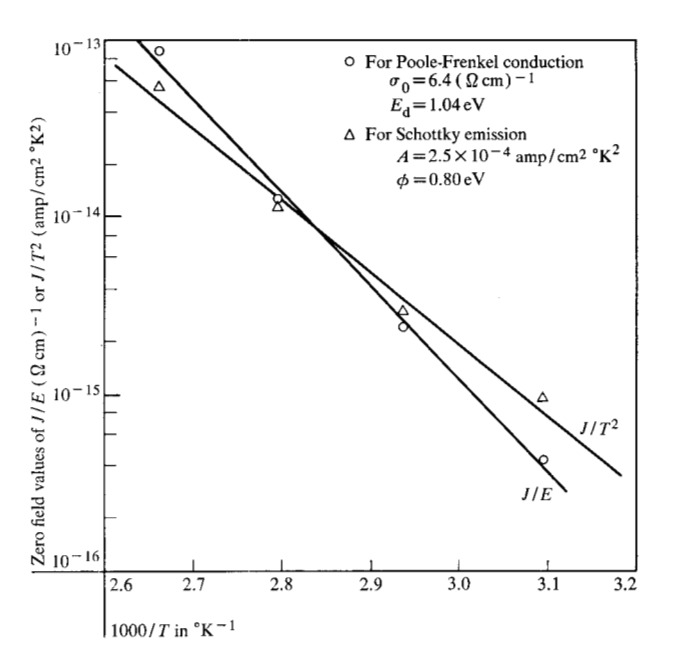


Figure 7 Zero-field conduction as a function of reciprocal temperature.

situation, partial compensation of donors by acceptors. They also calculated that σ_0 is given by

$$\sigma_0 = e\mu N_c \alpha, \tag{2}$$

where e is the electronic charge; μ , the mobility; N_e , the density of states in the conduction band; and α is a number greater or less than one, depending on the acceptor, donor and/or trap concentrations. In the free electron approximation the bulk values of mobility and effective mass⁵ yielded a value of

$$\sigma_0 \approx 2 \times 10^3 \ \alpha \ (\Omega\text{-cm})^{-1}$$
. (3)

A good fit to a plot such as Fig. 5 was no guarantee of Poole-Frenkel conduction. An equally good fit was obtained with a plot of log J vs. $E^{\frac{1}{2}}$, a test for Schottky emission. The relationship expected for Schottky emission is

$$J = AT^{2} \exp(-\phi/kT) \exp(\beta_{s} E^{\frac{1}{2}}/kT), \tag{4}$$

where $\beta_s = \frac{1}{2}\beta_{pf}$, ϕ is the barrier height, and A is a constant equal to 120 amp/cm²-°K². Poole-Frenkel conduction was distinguished from Schottky emission in two ways. First, the barrier height or trap depth was obtained from a plot of the zero-field intercepts vs. reciprocal temperature, Fig. 7. The constants determining the magnitude of the current density term were then derived and compared with theory. The empirical value obtained for σ_0 was 6 $(\Omega$ -cm)⁻¹; the value obtained for A was 2 \times 10⁻⁴ amp/cm²-°K². While it is not unusual for the empirical value of A to differ significantly from theory, a value six

691

^{*} The notation is conventional. T is the absolute temperature; k, Boltzmann's constant; ϵ_d is the trap depth below the conduction band; n is the index of refraction; E is the electric field; and J is the current density.

Table 2 Values of β_s and β_{pf} obtained by fittings Eqs. (1) and (4) to measured data,

T(°K)	$\beta_s(eV-cm^{1/2}-V^{-1/2})$	$\beta_{pf}(eV-cm^{1/2}-V^{-1/2})$
323	4.39 × 10 ⁻⁴	2.63 × 10 ⁻⁴
341	4.67×10^{-4}	2.72×10^{-4}
358	4.66×10^{-4}	2.84×10^{-4}
376	4.60×10^{-4}	2.78×10^{-4}

orders of magnitude too small was unreasonable. On the other hand, the empirical value for σ_0 required a value for α of 3 \times 10⁻³. This value was plausible if almost complete compensation of donors by acceptors occurred. ¹³ Consequently, the magnitude of the conduction strongly indicated a Poole-Frenkel mechanism.

The second test involved the magnitudes of β_* and β_{pf} . Table 2 gives the values obtained from least square fits of Eqs. (1) and (4) to the data.

From this analysis, Schottky emission required an index of refraction, $n=0.8\pm0.1$ and Poole-Frenkel conduction required $n=2.8\pm0.1$. Cardona¹⁵ found that in bulk SrTiO₃, n varied from 2.3 to about 2.6 across the visible spectrum. Furthermore, the index of refraction in these films was measured crudely by the Abeles technique¹⁶ and found to be about 2.4. Thus, the data again pointed strongly to Poole-Frenkel conduction in the forward direction. As final proof of this, even though the low field conductivity of various films varied by almost an order of magnitude, the value of β_{pf} remained $\approx 2.7 \times 10^{-4}$ eV-cm³-V⁻³.

The currents in the reverse direction (Fig. 6) were not so easily understood. Certainly, their asymmetry ruled out the contact-independent Poole-Frenkel conduction. Au was known¹⁷ to make a highly blocking contact to SrTiO₃. Furthermore, for a similar material, BaTiO₃, the Cu barrier was much lower than the Au barrier.¹⁸ Therefore, the asymmetry seen in the *J-E* characteristic could reasonably be ascribed to a contact effect. However, from the similarities between the forward and reverse characteristics, it was apparent that the reverse current was not compatible with Schottky emission either. In particular, the current density was more than seven orders of magnitude too small to be consistent with the low activation energy.

The slow transient currents observed when the voltage was first applied indicated a charging of the Au-SrTiO₃ barrier. For reverse polarities this was probably accomplished by the emptying of traps, very likely the same traps responsible for conduction in the forward direction. Judging from the high impurity concentration in the cathode, we observe that the positive charge density resulting

from empty traps could have been as high as $10^{20}/\text{cm}^3$. If it is assumed that the charge applied to the film was localized in the barrier region, the fields applied to the barrier could than have been as high as $5 \times 10^6 \text{V/cm}$. According to Tantraporn, ¹⁴ this is in a transitional region between Schottky emission and tunneling, where no simple approximate formula for the conduction is available.

It is also possible to explain the reverse conduction in terms of tunneling from the Au conduction band directly into the traps. This is an attractive hypothesis, for it avoids the necessity of very high barrier fields. As will be discussed below, the dielectric constant was a strong function of the applied field. But this dependence was not a function of the field direction, and some dependence on field direction would have been observed if the fields were highly non-uniform in one direction.

• Heat treatment and electrode effects

When Mo was used for the final electrode in place of Cu, the leakage current was increased by about two orders of magnitude in each direction. This seems inconsistent with the preceding analysis, in that trap-limited conduction should not have been electrode dependent. However, heat treatment experiments provided an explanation. The experiments were performed as follows: Devices contacted by Mo top electrodes and devices contacted by Cu top electrodes were overcoated with sputtered 7059 glass; holes were etched through these glass films to the electrodes and a final layer of Mo-Au was deposited and etched to provide contacts to the capacitor structure. The resulting passivated devices were then subjected to heat treatment in air at 380°C. The changes in leakage current are shown in Fig. 8 for a negative potential on the Mo and Cu. The behavior was similar for positive potentials, although the asymmetry remained.

The explanation of the heat treatment effects is that Mo, but not Cu, tended to reduce the SrTiO₃. The rate of formation of molybdenum oxide decreased as its thickness increased, until oxygen diffusion through the glass overcoat was able to replenish the oxygen being removed from the SrTiO₃ by the Mo. That the outside ambient was critical was established by a further short heat treatment in forming gas of the device with the Mo electrode; this raised the leakage current well above the peak value observed during the heat treatment in air. Significantly, the low frequency dielectric loss in heat treated devices with Mo electrodes was far higher than that shown in Fig. 4. Furthermore, the dielectric constant of devices with a Mo electrode was decreased more than 10% by the heat treatment.

• Dependence of κ on electric field

Devonshire, ¹⁹ and later Slater, ²⁰ developed theories which provide guidance for the expected dependence of the

dielectric constant on electric field. For a cubic crystal their expressions relating polarization to the electric field applied in a particular direction have the form:

$$E_x = aP_x + bP_x^3 + cP_x^5 + \cdots, (5)$$

where cross terms are neglected because the crystal is isotropic. The higher order terms are due to the anharmonic lattice potential. Although the fifth order term is usually neglected, this term becomes important at the very high fields applied to these films. Inverting Eq. (5) to express the polarization as a power series in the field gives

$$P_x = (1/a)E_x - (b/a^4)E_x^3 + [(3b^2/a^7) - (c/a^6)]E_x^5 - \cdots$$
(6)

The small signal κ is defined by

$$\kappa = 1 + 4\pi \, dP_x/dE_z. \tag{7}$$

If Eq. 5 is differentiated with respect to E_x and combined with Eqs. (6) and (7), the result can be put in the form

$$\kappa = 1 + \frac{4\pi}{a} \left[1 + \frac{3b}{a^3} E_x^2 - \left(\frac{6b^2}{a^6} - \frac{5c}{a^5} \right) E_x^4 + \cdots \right]^{-1}.$$
 (8)

This is very similar to an expression given by Rupprecht et al.,²¹ except that Eq. (8) does not neglect the fourth order field dependence. In Ref. 22 the values for $4\pi/a$ and $3b/a^3$ were obtained from measurements on bulk crystals. At 25°C, $4\pi/a$ is essentially equal to 310, the dielectric constant at zero field.² The other terms which can be evaluated²¹ are (at 25°C):

For the [100] direction (strongest field dependence):

$$3b/a^3 = 3.68 \times 10^{-12} \text{ cm}^2/\text{V}^2;$$

 $6b^2/a^6 = 9.0 \times 10^{-24} \text{ cm}^4/\text{V}^4.$ (9)

For the [111] direction (weakest field dependence):

$$3b/a^3 = 2.21 \times 10^{-12} \text{ cm}^2/\text{V}^2;$$

 $6b^2/a^6 = 3.24 \times 10^{-24} \text{ cm}^4/\text{V}^4.$

The dependence of κ on electric field for various films is given in Fig. 9. The measurements were made using a P. A. R. Model JB-6 lock-in amplifier in conjunction with a recorder. The dashed lines in this figure were obtained by extrapolating the empirically fitted expression given in Ref. 21. Therefore, the dashed lines were calculated without the fourth order field dependence, a neglect that is probably not justified. The fields applied to these films were as much as five times the breakdown field of bulk $SrTiO_3$.²² The term, $(6b^2/a^6)E_x^4$ in Eq. (8) (which is negligible for the fields applied to the bulk material) is actually larger at 10^6 V/cm than the second order term,

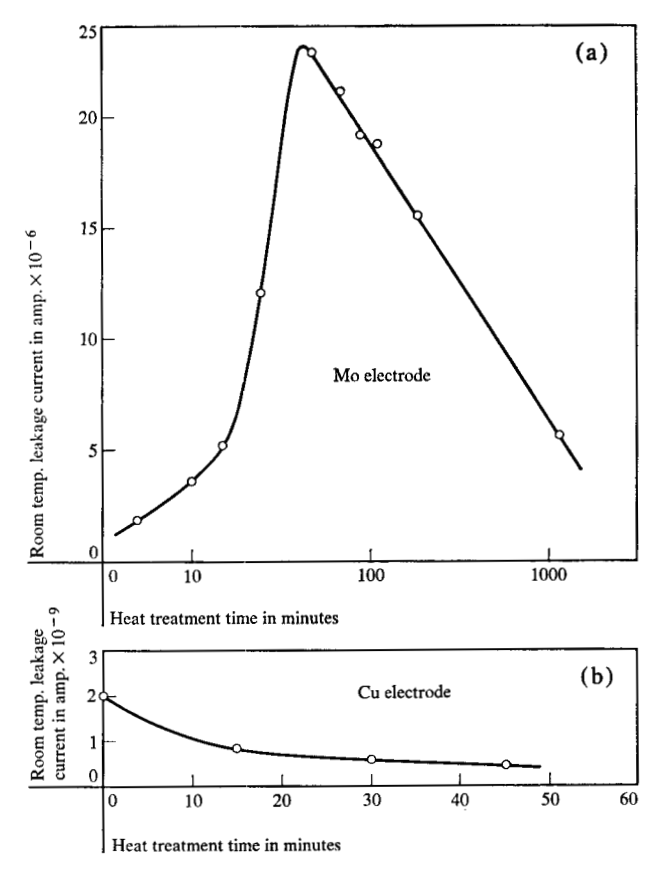
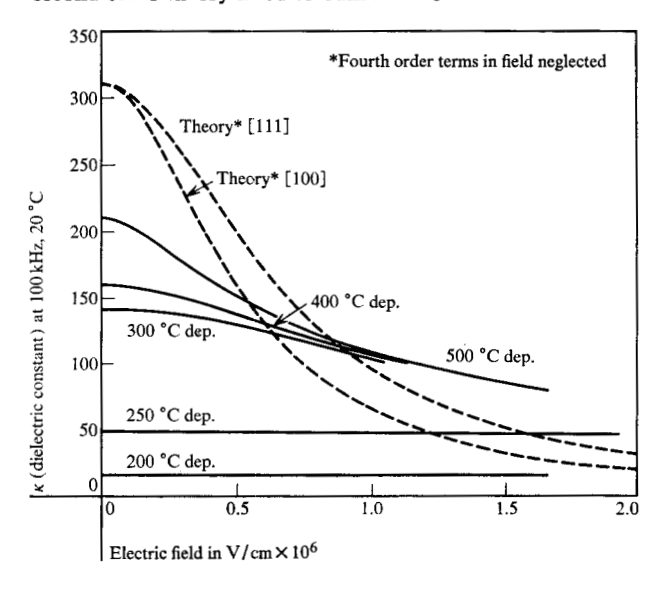


Figure 8 Effect of heat treatment on room temperature conduction through a 3000-Å film. Device areas, about 2 × 10⁻³ cm² each. (a) Mo-SrTiO₃-Au; (b) Cu-SrTiO₃-Au.

Figure 9 Dielectric constant κ vs. electric field; films and second order theory fitted to bulk SrTiO₈.



 $(3b/a^3)E_x^2$. Therefore, unless the two fourth order terms exactly cancel (an unlikely event), the fourth order dependence can not be neglected at these fields.

The trend of the data in Fig. 9 supports this conclusion. If fields above 10^6 V/cm could be applied to bulk SrTiO₃, it seems likely that its κ would remain higher than, but would closely approach, the κ of the film deposited at 500°C. If so, the difference between this κ and that calculated from second order theory would require partial, but not complete, cancellation of the fourth order terms.

A few questions remain regarding the above interpretation. At high fields the expansion of the field in a power series such as Eq. (5) may not be valid. Also, the data may have been influenced by non-uniform fields caused by stored charge in the dielectric. However, the κ -E curves were essentially independent of polarity, except for effects of the order of 0.1% at low fields. Therefore, any non-uniformity in the electric field must have been small.

While the κ -E curves were essentially independent of polarity, the very small effects seen at low fields were interesting from another standpoint. They add support to some of the concepts discussed earlier. With Cu as the top electrode, the maximum in κ occurred not at zero field, but at ± 0.5 volts applied to the Au. The κ -E curve was not strictly symmetric about this point, but had a region of nearly constant slope at small negative voltages on the Au. With Mo as the top electrode the κ -E curve had a distinct double peak, and was symmetric around the zero field point within ± 0.1 volts. For both electrodes a very small and slow time dependent drift was observed, making the κ -E curves a function of the previous history of applied field.

The dependence on electrodes and the asymmetry were approximately consistent with the work function differences between the various metals. The time dependence and the double peak were evidence of trapped charge and electric fields at the electrode barriers. Since the effects were so small, however, higher order anharmonic terms in the lattice potential still appear to be necessary to explain the high field κ -E curves.

The decrease in sensitivity of κ to electric fields in the films deposited at lower temperatures was very likely related to the decrease in κ itself. This variation in κ with grain size was also reported for BaTiO₃ films.²³ The cause of these effects probably lies in the disordering of the lattice by the grain boundaries.

Conclusions

Although the properties of the films varied in fairly complex ways, only two significant factors were found that influenced these properties: oxygen vacancy concentration and crystallite size. In turn, these two factors were initially established by two sputtering parameters, oxygen partial pressure and deposition temperature. The

oxygen vacancy concentration was, however, easily influenced by those subsequent processing steps which provided a reducing environment. Oxygen partial pressure during sputtering proved difficult to control. The difficulty arose because of a reaction between oxygen and hydrocarbons adsorbed on the walls of the sputtering chamber. It was necessary to add approximately 5% oxygen to the argon to overcome this problem and obtain insulating films.

In many ways the films closely resembled bulk SrTiO₃. The conductivity of the highest resistivity films was probably determined by impurities in the cathode material. but the influence of oxygen on film conductivity certainly paralleled its influence on conduction in bulk SrTiO₃. Gold made a blocking contact to the films, as it does to the bulk material. The barrier between Cu and SrTiO₃ was lower than that between Au and SrTiO₃, as expected. The index of refraction was approximately the same as that of bulk. Dielectric loss was larger, but at least partly understandable in terms of bulk properties. The dielectric constant was, at best, about 65% of the value given for bulk single crystal SrTiO3. However, values reported for the dielectric constant of bulk ceramic SrTiO₃ are also lower.²⁴ The influence of electric field on the dielectric constant was qualitatively in agreement with measurements of bulk crystals, although higher order anharmonic terms in the lattice potential were required to explain the high field effects.

Although the conduction in the highly oxidized films was probably not an intrinsic property of SrTiO₃, it is interesting that so clear a choice could be made between Poole-Frenkel conduction and Schottky emission. The data provided a striking example of the need to use the high frequency dielectric constant in the theory of Poole-Frenkel conduction.¹²

Acknowledgments

E. D. Alley was almost completely responsible for the operation of the sputtering system. L. I. Maissel and P. D. Davidse were most helpful during the design of this system. The use of rf sputtering for the deposition of high dielectric constant insulators was suggested by H. Caswell. C. Aliotta supplied the electron micrographs, G. Schlig performed the pulse measurements, and E. Stern provided helpful criticism during the preparation of this manuscript.

References

- 1. R. W. G. Wyckoff, Crystal Structures, Interscience Publishers, Inc., New York 1948, Chap. VII.
- 2. A. Linz, Phys. Rev. 91, 753 (1953).
- 3. W. G. Spitzer et al, *Phys. Rev.* **126**, 1710 (1962).
- A. von Hippel and W. B. Westphal, Tech. Rep. 145, Laboratory for Insulation Research, Mass. Inst. Tech., Dec. 1959
- 5. H. P. R. Frederikse et al., Phys. Rev. 134, A442 (1964).

- 6. P. D. Davidse and L. I. Maissel, J. Appl. Phys. 37, 574 (1966).
- 7. Rare Metals Handbook, C. A. Hampel, Ed., Reinhold Publishing Corp., London 1961, p. 183.
- 8. H. Salmang, Ceramics, Butterworths, London 1961, p. 358.
- 9. W. B. Pennebaker, J. Appl. Phys. 40, 394 (1969).
- 10. R. H. Tradgold and R. H. Williams (Proc. Eighth Conf. on the Physics of Semiconductors, Kyoto) J.
- Phys. Soc. Japan 21, Suppl. No. 46-50 (1966).
 11. A. E. Paladino, L. G. Rubin and J. S. Waugh, J. Phys. Chem. Solids 26, 391 (1965).
- 12. J. Frenkel, Phys. Rev. 54, 647 (1968).
- 13. P. Mark and T. Hartman, J. Appl. Phys. 39, 2163 (1968).
- 14. W. Tantraporn, Sol. St. Elect. 7, 81 (1964).
- 15. M. Cardona, Phys. Rev. 140, A651 (1965).
- 16. L. Young, Anodic Oxide Films, Academic Press, Inc., London and New York 1961.

- 17. J. Carnes and A. Goodman, J. Appl. Phys. 38, 3091 (1967).
- T. Murankani, J. Phys. Soc. Japan 24, 282 (1968).
 A. F. Devonshire, Phil. Mag. (Series 7) 40, 1040 (1949).
- 20. J. C. Slater, Phys. Rev. 78, 748 (1950).
- 21. G. Rupprecht, R. O. Bell and B. D. Silverman, Phys. Rev. 123, 97 (1961).
- 22. H. Barrett, J. Appl. Phys. 35, 1420 (1964).
- 23. E. K. Müller, B. J. Nicholson and M. H. Francombe, Electrochem. Tech. 1, 158 (1963).
- 24. P. A. Larssen, Insulation 13, 316 (1967).
- 25. J. A. Becker, E. J. Becker and R. G. Brandes, J. Appl. Phys. 32, 411 (1961).

Received March 7, 1969